CMS Draft Analysis Note

The content of this note is intended for CMS internal use and distribution only

2013/06/05
Head Id: 188785
Archive Id: 188879
Archive Date: 2013/06/05
Archive Tag: trunk

Angular coefficients measurements in DY events

Matthew Jones[1], David Silvers[1], Arie Bodek[2], Jiyeon Han[2??]

[1] Purdue University
[2] University of Rochester

DRAFT

Abstract

We report on the first measurement of the angular distributions of final state lepton in $pp \to \gamma^*/Z \to \mu^+\mu^-$ events produced in the Z boson mass region ($60 < M_{ee} < 120$ GeV/c^2) at $\sqrt{s} = 7$ TeV. The data sample collected by the CMS detector corresponds to 4.9 fb^{-1} of integrated luminosity. The transverse momentum dependence of angular coefficients A_0, A_1, A_2, A_3, and A_4 are compared with POWHEG Monte Carlo generators based on Quantum Chromodynamics (QCD). The transverse momentum dependence of A_0 is in agreement with the predictions of perturbative QCD, but A_2 is lower than the prediction at large transverse momentum proceeds via a combination of the quark-antiquark annihilation and the quark-gluon Compton processes.

This box is only visible in draft mode. Please make sure the values below make sense.

PDFAuthor: Matthew Jones, David Silvers, Arie Bodek, Jiyeon Han
PDFTitle: Angular coefficients measurements in DY events
PDFSubject: CMS
PDFKeywords: CMS, physics, SMP

Please also verify that the abstract does not use any user defined symbols

DRAFT

1 Introduction

The angular distribution of the final state muon in the quark-antiquark ($q\bar{q}$) annihilation process $q\bar{q} \to \gamma^*/Z \to \mu^+\mu^-$ can be written as

$$\frac{d\sigma}{dcos\theta} \propto (1 + cos^2\theta) + B\ cos\theta.$$

When quarks are bound in a nucleon (e.g. $pp \to \gamma^*/Z \to \mu^+\mu^-\ X$), the γ^*/Z is in general produced with a finite transverse momentum. In Quantum Chromodynamics (QCD) at leading order (LO) this occurs either through the annihilation process with a gluon (g) in the final state ($q\bar{q} \to \gamma^*/Z\ g$), or via the Compton process with a quark in the final state ($qg \to \gamma^*/Z\ q$), as shown in figure 1. The general expression[1] for angular distribution of the final state electron in the Collins-Soper(CS) frame[2] is given by:

$$\begin{aligned}\frac{d\sigma}{d\cos\theta d\phi} &\propto (1+\cos^2\theta) + \frac{1}{2}A_0(1-3\cos^2\theta) + A_1\sin 2\theta\cos\phi + \frac{1}{2}A_2\sin^2\theta\cos 2\phi \\ &+ A_3\sin\theta\cos\phi + A_4\cos\theta + A_5\sin^2\theta\sin 2\phi + A_6\sin 2\theta\sin\phi + A_7\sin\theta\sin\phi.\end{aligned}$$

Here, θ and ϕ are the polar and azimuthal angles of the muon in the CS frame. The angular coefficients $A_0 - A_7$ are in general functions of the invariant mass $M_{\ell\ell}$, rapidity y, and transverse momentum P_T of the dilepton in the lab frame[3].

When integrated over ϕ the differential cross section reduces to:

$$\frac{d\sigma}{d\cos\theta} \propto (1+\cos^2\theta) + \frac{1}{2}A_0(1-3\cos^2\theta) + A_4\cos\theta \tag{1}$$

When integrated over $cos\theta$, the differential cross section reduces to:

$$\frac{d\sigma}{d\phi} \propto 1 + \beta_3\cos\phi + \beta_2\cos 2\phi + \beta_7\sin\phi + \beta_5\sin 2\phi \tag{2}$$

$$\beta_3 = \frac{3\pi A_3}{16},\ \beta_2 = \frac{A_2}{4}, \beta_7 = \frac{3\pi A_7}{16},\ \beta_5 = \frac{A_5}{4}.$$

The A_1 and A_6 terms vanish when the differential cross section is integrated over $\cos\theta$, or ϕ, respectively.

Calculations which are based on perturbative QCD (pQCD) make definite predictions for all of the angular coefficients. For $pp \to \gamma^*/Z \to \mu^+\mu^-\ X$ the angular coefficients A_5, A_6 and A_7 are close to zero [1], and if we integrate over positive and negative y, the angular coefficients A_1 and A_3 are small. We can use equation 1 to extract A_0 and A_4 and equation 3 to extract A_2 and A_3 under the assumption that A_5 and A_7 are zero (as is theoretically expected).

For the $q\bar{q} \to \gamma^*/Z\ g$ annihilation process [4–7], pQCD in LO predicts that the angular coefficients A_0 and A_2 are equal, independent of Parton Distribution Functions (PDFs), or y, and are described by $A_0^{q\bar{q}} = A_2^{q\bar{q}} = \frac{P_T^2}{M_{\ell\ell}^2 + P_T^2}$.

For the $qg \to \gamma^*/Z\ q$ Compton process, A_0 and A_2 depend on PDFs and y. However, in pQCD at LO, when averaged over y, A_0 and A_2 are approximately [8, 9] described by $A_0^{qg} = A_2^{qg} \approx \frac{5P_T^2}{M_{\ell\ell}^2 + 5P_T^2}$.

In this analysis, we measure the angular coefficients using 2 dimentional fitting method which measures full angular coefficients from A_0 to A_7 in terms of the trnasverse momentum (P_T) and rapidity (y). The measured angular coefficients, A_0, A_2, A_3, and A_4, are confirmed by 1 dimentinal fitting method integrating over $\cos\theta$, or ϕ.

DRAFT

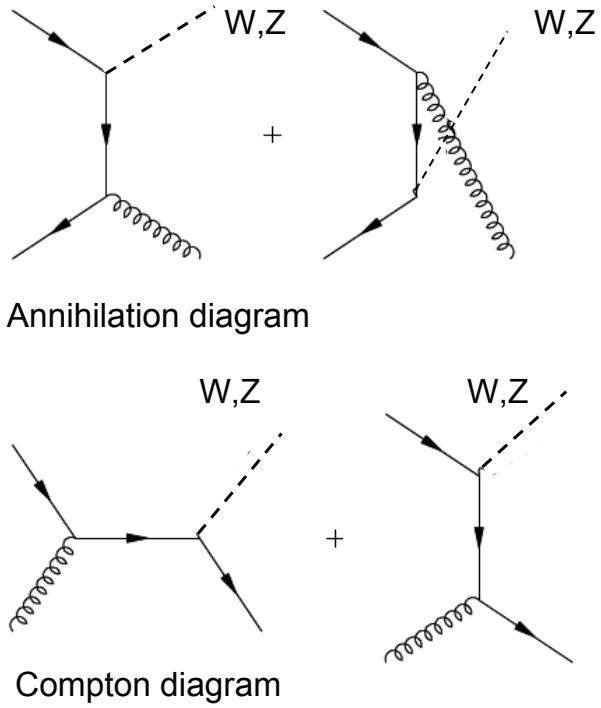

Figure 1: Leading order annihilation ($q\bar{q} \to \gamma^*/Z\ g$) and Compton ($qg \to \gamma^*/Z\ q$) diagrams for the production of Z bosons with finite transverse momentum

2 Data set and Event selection

The analysis is performed using the full data sample collected at $\sqrt{s}$ = 7 TeV (2011) which corresponds to 4.9 fb^{-1} of the integrated luminosity. We use the double muon trigger sample which has asymmetric p_T threshold, HLT_Mu17_Mu8, to select dimuon candidates. To clean up the sample, the muon selection criteria is required and this selection is defined as a tight muon selection in CMS muon POG recommendation.

Specifically, the selection criteria are following :

- HLT Mu17_Mu8 (available after run = 165970)
- muon p_T >20 GeV and detector $|\eta| < 2.4$
- Muon selection : Tight muon selection is applied
- Global and Tracker Muon
- Global muon normalized fit $\chi^2 < 10$
- Number of Tracker hits greater than 10
- At least one muon chamber hit included in the global-muon track fit
- Number of pixel hits greater than or equal to 1
- Number of muon stations greater than or equal to 2
- $dxy < 0.2$
- Fractional tracker isolation : $TrkIso_{\Delta R<0.3}/P_T < 0.1$
- Mass and rapidity selection : $60 < M_{\mu^+\mu^-} < 120\ GeV/c^2$ and $|y| < 2.4$
- Select di-muon pairs from events with only one di-muon candidate

DRAFT

(Event fraction which has more than one di-muon pairs is less than 0.008%)

In the analysis, we restrict the kinematic range, $60 < M_{\mu^+\mu^-} < 120\ GeV/c^2$ and $|y| < 2.4$. Since the muon detector covers up to $|\eta| < 2.4$ which is relevant to $|y| < 2.4$, we only measure the angular coefficients in $|y| < 2.4$ where the events can be found in the detector. In the event selection, we reject the events which have the multiple Z candidates which has a negligible effect. (the event fraction which has multiple Z cadidates in the event is less than 0.008%.) After all event selection, we find ~ 1.78 M Z candidates.

The data sample used for the analysis is produced in CMSSW 4_2_x version. The produced data has the detector mis-alignment bias which affects the muon momentum. We applied the muon momentum correction (Rochester correction) in data and MC, which improves the determination of the muon momentum and reduces its dependence on the muon charge, η, and ϕ. More details of the muon momentum correction will be discussed later. For MC, we use *POWHEG* Monte Carlo sample which has Pythia parton showering. The MC sample is also produced CMSSW 4_2_x version (Fall11-PU_S6_START42). Table 1 summarizes the data and MC sample used for the analysis.

Table 1: The data and MC sample used for the analysis.

Data	
Path	Integrated luminosity
/DoubleMu/Run2011A-PromptReco-v4/	0.84 fb^{-1}
/DoubleMu/Run2011A-05Aug-v1/	0.48 fb^{-1}
/DoubleMu/Run2011A-PromptReco-v6/	0.72 fb^{-1}
/DoubleMu/Run2011B-PromptReco-v1/	2.86 fb^{-1}
Total luminosity	4.90 fb^{-1}
MC	
/DYToMuMu_M-20_CT10_TuneZ2_7TeV-powheg-pythia/ Fall11-PU_S6_START42_V14B-v1	

3 Analysis procedure

The analysis is done in seven bins of transverse momentum (P_T bins : (0,10), (10,20), (20,35), (35,55), (55,80), (80,120), and (120,200)) for two rapidity bins ($|y| < 1.0$ and $1.0 \leq |y| < 2.4$). PDFs and the dilution effect changes in the rapidity, so the measurement in $|y|$ provides better understanding of the mechanism.

The determination of the detector acceptance require that the various kinematic distribution in the MC agree with the data. Specifically, these include the rapidity distributions and the transverse momentum distributions. In general, weighting factors to correct the kinematic distribution in MC are extracted from the ratio of data to MC in the reconstructed level. The weighting factors are then applied to the MC to ensure that the various kinematic distributions in the weighted MC are the same as in data. Since Powheg prediction doesn't describe data well for Z P_T distribution, an additional tuning for Z P_T distribution is required. The reconstructed Z P_T distribution is compared between data and MC and its ratio is used as the correction factor. The correction factor is applied to MC as the event weighting in the generated Z P_T distribution. The procedure is iterated until the ratio of data to MC is flat. Figure 2 shows the correction factor for Z P_T distribution. The data-driven Z P_T correction factor is compared with the correction factor derived from MadGraph and the difference is assigned as a systematic uncertainty for Z P_T modeling.

DRAFT

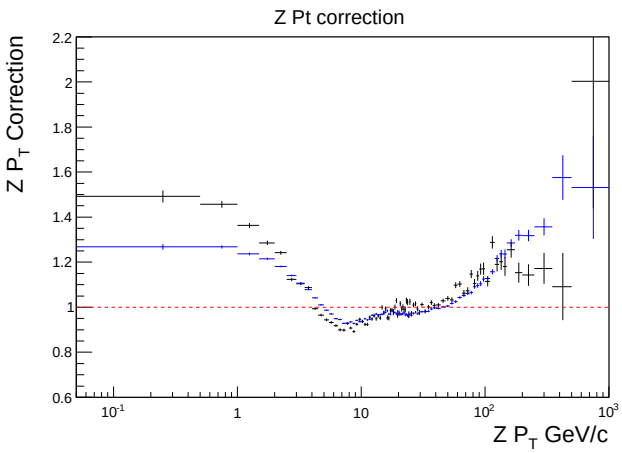

Figure 2: Z P_T correction factor. The black points are the correction factor derived by the data-driven method and the blue points are the correction derived by MadGraph prediction. The difference between the data-driven correction vs. MadGraph correction is assigned as a systematic uncertainty of Z P_T modeling.

3.1 Muon Momentum Scale : Rochester correction

A muon momentum correction([10] [11] [12]) is applied to compensate for misalignment of the CMS detector. The primary cause of bias in the reconstructed momentum is the misalignment of the tracker. The tracker geometry is not well modeled in both data and MC and the bias is different between data and MC.

To remove the bias, the muon momentum correction is extracted using the average of $1/p_T$ (i.e. $< 1/p_T >$) spectra of muons from Z decays in the bins of muon charge (Q), θ, and ϕ. On top of $< 1/p_T >$ correction, we extract the additional correction factors using the average of Z mass, $< M^Z_{\mu\mu} >$, in η and ϕ bin of μ^+ or μ^-. The Z mass is less sensitive to the efficiencies, background, and modeling of kinematic distributions. Therefore, the additional correction using Z mass reduces the systematic uncertainty of the correction. This additional correction from Z mass is also propagated into $< 1/p_T >$ correction at the end.

Before the muon momentum correction, the ϕ distribution of Z bosons in the Collins-Soper Frame showed unphysical features that indicated a a bias in reconstruction of positive and negative muons. After the application of the momentum corrections to the data and MC, it removes the bias from a misalignment and also an possible error in the integral of B*dL.

3.2 Efficiencies

3.2.1 Trigger Efficiency

The double muon trigger sample passed HLT_Mu17_Mu8 is used to select di-muon candidates. This trigger path only requires muon p_T threshold, so the trigger efficiency is relatively high in high muon p_T events ($p_T > 20$ GeV) decaying from Drell-Yan process. The trigger efficiency (ϵ^{μ}_{trig}) for each trigger filter, $Mu17$ or $Mu8$, is measured using the tag-and-probe method, respectively. To reduce the background contamination in sample, we apply all muon ID cuts on both the tagged and probe legs. To minimize the trigger bias, SingleMu trigger sample (HLT_IsoMu24) is used to measure the trigger efficiency. The trigger match for HLT_IsoMu24 is required for the tagged leg and the probe leg is used to measure the trigger efficiency. The high pile-up data (2011B) has a lower trigger efficiency, so we measure the trigger efficiency for

DRAFT

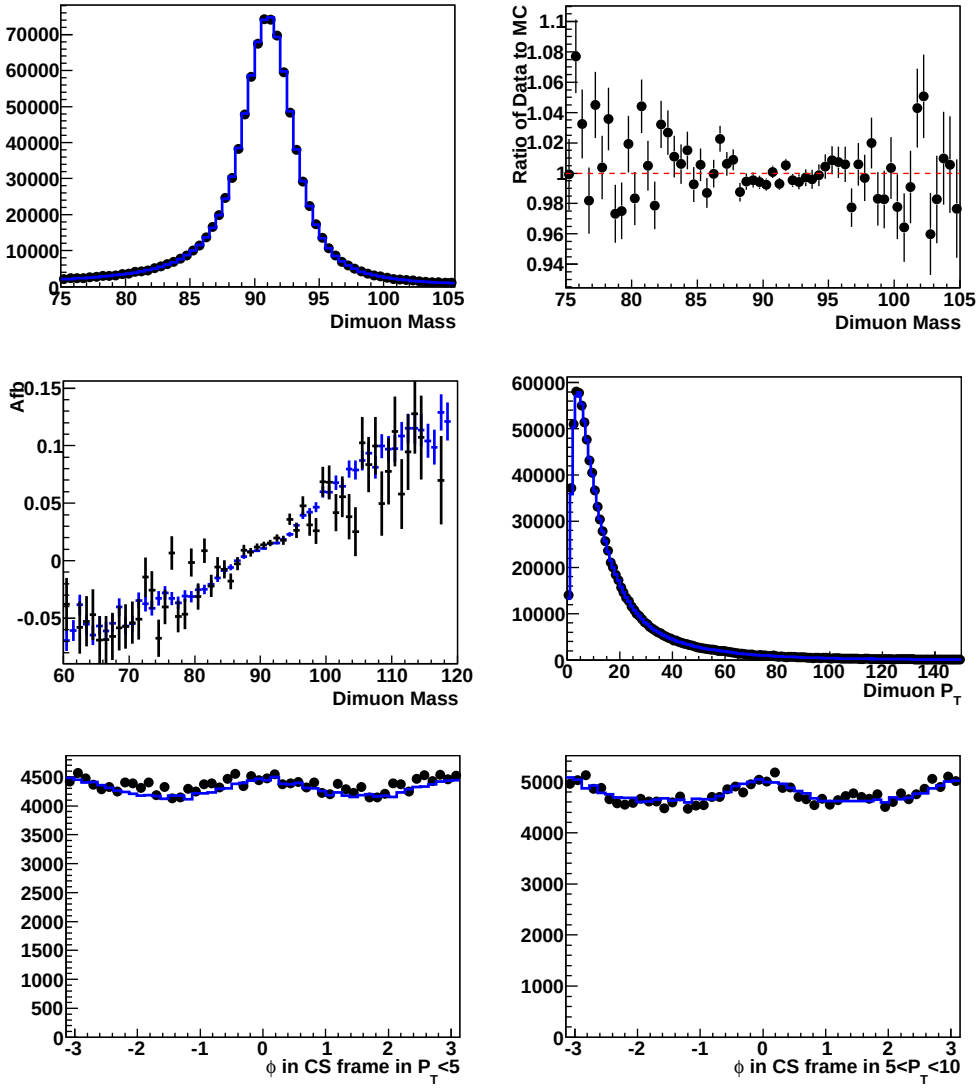

Figure 3: The first reference plot of the muon momentun correction after the correction in 2011A data : Z mass, A_{FB}, Z P_T, and ϕ in Collins-soper frame in low Z P_T. The plots in the first row show the dimuon distribution in data (black) and MC (blue) and its ratio. The plot in the left side of the second row shows the forward-backward asymmetry and the plot in the right side shows Z P_T distribution. The Z P_T distribution in MC is tuned to match the data. The plots in the bottom show ϕ distribution in Collins-soper frame in Z $P_T < 5$ (left) , $5 < Z$ $P_T < 10$ GeV/c (right). The black points corresponds to data and the blue to MC.

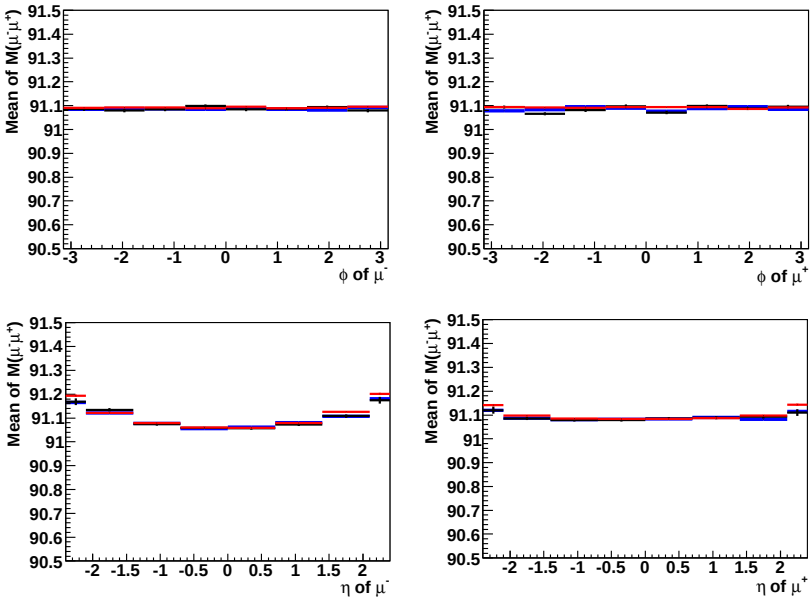

Figure 4: The second reference plot of the muon momentum correction after correction in 2011A data: Z mass profile in muon ϕ and η. The plots in top show the Z mass profile in ϕ of μ^- (left) and μ^+ (right) and the plots in bottom show the Z mass profile in η of μ^- (left) and μ^+ (right). The Z mass corresponds to the average of Z mass in the range of $86.5 < M(\mu\mu) < 96.5\,\mathrm{GeV}/c^2$. The black points are data, the blue points are MC, and the red points are the generated level after QED radiation which is used as the reference point.

2011A and 2011B data separately.

The trigger efficiency is relatively flat as a function of muon p_T for $p_T > 20$ GeV/c, but may have a small η and ϕ dependence. The trigger efficiency is measured in terms of muon η and ϕ and the η and ϕ dependence of the this trigger efficiency (for single muon object) is shown in Figure 5 and 6.

For dimuon events, either of two muons needs to pass HLT_Mu8 and another should pass HLT_Mu17. We measure the trigger efficiency of HLT_Mu8 (ϵ^{μ}_{trig8}) and HLT_Mu17 on top of HLT_Mu8 requirement ($\epsilon^{\mu}_{trig17|8}$) and propagate the trigger efficiency of the event ($\epsilon^{2\mu}_{trig}$) following :

$$\epsilon^{2\mu}_{trig} = \epsilon^{\mu}_{trig8}(\eta_1,\phi_1) \times \epsilon^{\mu}_{trig8}(\eta_2,\phi_2) \times (1.0 - (1.0 - \epsilon^{\mu}_{trig17|8}(\eta_1,\phi_1)) \times (1.0 - \epsilon^{\mu}_{trig17|8}(\eta_2,\phi_2))). \quad (3)$$

3.2.2 Muon Reconstruction Efficiency

We need to make sure that the muon selection efficiency is correctly described in the MC. This is accomplished by applying scale factors to the efficiency in the Monte Carlo to make sure that they match the data. The muon identification selection described in section 2 is applied to select the muon object and remove backgrounds. The muon reconstruction efficiency is measured using the tag-and-probe method as a function of muon η and ϕ as defined in the trigger efficiency. The tagged and probe leg is randomized based on muon p_T to reduce the bias, so on average, the p_T spectrum of both tag and probe legs is the same.

DRAFT

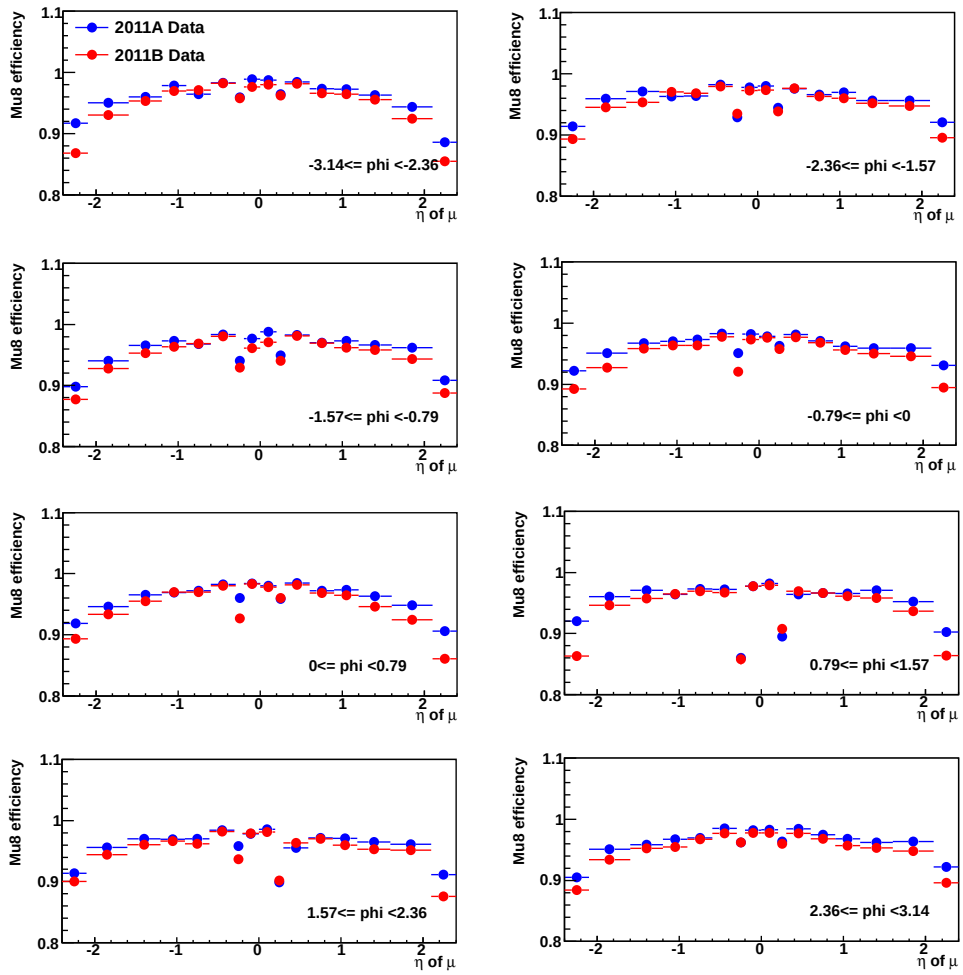

Figure 5: The single muon trigger efficiency ϵ^{μ}_{trig8} as a function of muon η and ϕ. The blue points are for 2011A data and the red points are for 2011B data.

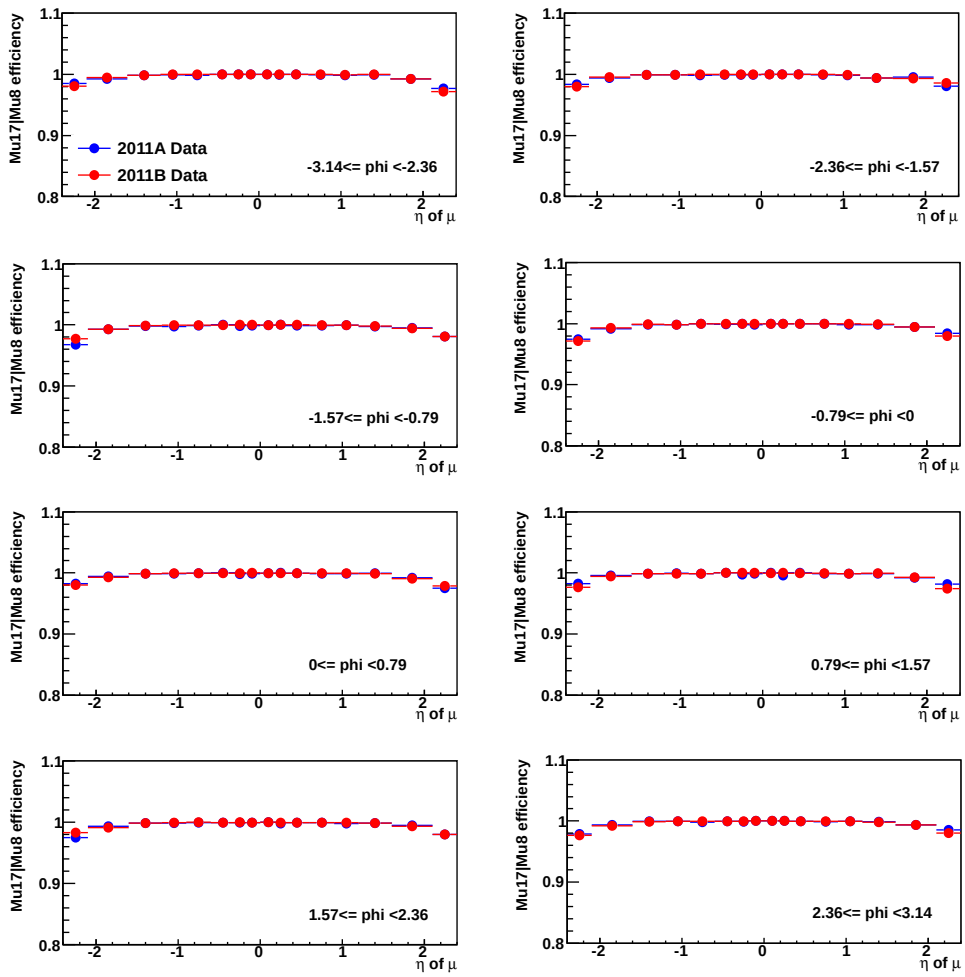

Figure 6: The single muon trigger efficiency $\epsilon^{\mu}_{trig17|8}$ as a function of muon η and ϕ. The blue points are for 2011A data and the red points are for 2011B data.

The muon reconstruction efficiency is parameterized to

$$\epsilon_{recon} = \epsilon_{tracking} \times \epsilon_{global} \times \epsilon_{ID} \times \epsilon_{iso} \tag{4}$$

The tagged leg is required to pass all muon ID selection to clean up the sample and also to be matched to the triggered object to remove trigger bias when measuring the muon reconstruction efficiency from the data.

The tracking efficiency is $\sim$ 100 % and the scale factor of data to MC is close to 1.0, so the tracking efficiency is excluded in the parameterization of the muon reconstruction efficiency. A general track is used as a probe to measure the global muon reconstruction efficiency. For the ID efficiency, a global muon is used as a probe and required to pass the tight muon selection criteria described in Section 2. The fractional track isolation cut ($Iso_{track}/p_T < 0.1$) efficiency used for the analysis is also measured with ID efficiency together.

In the measurement of the muon reconstruction efficiency, the probe leg is required to pass the kinematic selection ($P_T > 20$ GeV/c and $|\eta| < 2.4$) and the efficiency is defined following :

$$\epsilon(\eta, \phi) = \frac{N_{pass}(\eta, \phi)}{(N_{pass}(\eta, \phi) + N_{fail}(\eta, \phi))} \tag{5}$$

Here, N_{pass} is the number of events passing the selection for the probe leg, and N_{fail} is the number of events failed the selection for the probe leg. The background is estimated using the Z mass fitting method. The convolution of Briet-Wigner and Gaussian function is used as the signal and the exponential function is used as the background shape. The mass window, $60 < M_{\mu\mu} < 120\,\mathrm{GeV}/c^2$ is used for the efficiency study. Figure 7 and 8 show the total efficiency and its ratio as a function of muon η and ϕ. The efficiency scale factor in η and ϕ is implemented into MC by using event weights.

After applying the corrections, we compare the kinematic distributions of Z boson between data and MC. Figures 9 and 10 show a comparison of various kinematic distributions between the data and MC before the background subtraction.

In the top part of Figure 9 we show a comparison of the invariant mass (left) and boson rapidity (right) distributions between the data (black) and MC (blue). In the bottom part we show a comparison of the boson P_T (left) and NVertices (right) distributions between the data (black) and MC (blue).

In Figure 10 we show a comparison of the $\cos\theta$ (left) and ϕ (right) distributions in the Collins-Soper frame between the data (black) and MC (blue) used for the angular coefficients measurement.

There is a good agreement between data and MC for the various kinematic distributions of the events.

3.3 Background Estimation

The dominant backgrounds which pass the selection cuts come from $t\bar{t}$, $\gamma^*/Z \to \tau\tau$, and diboson (WW, WZ, ZZ) production, while tW, single W, and QCD are smaller background processes. We use the data-driven $e\mu$ method to estimate these backgrounds.

The data-driven $e\mu$ background estimation process is possible due to the fact that many of the background processes which decay to two muons in the final state can also decay to an electron and muon in the final state.

DRAFT

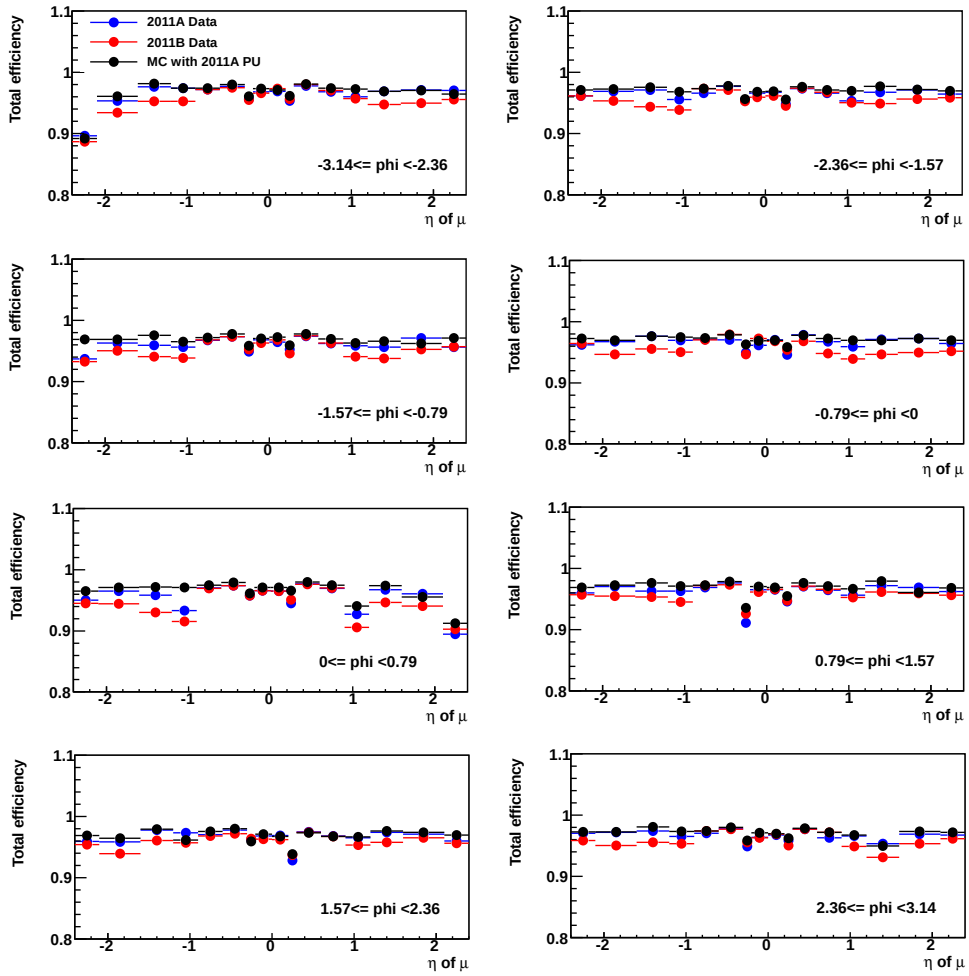

Figure 7: The total (global x ID x Iso) efficiency as a function of η for each ϕ bin. The blue points are the efficiency for 2011A data, and the red points are for 2011B, and the black points are for MC.

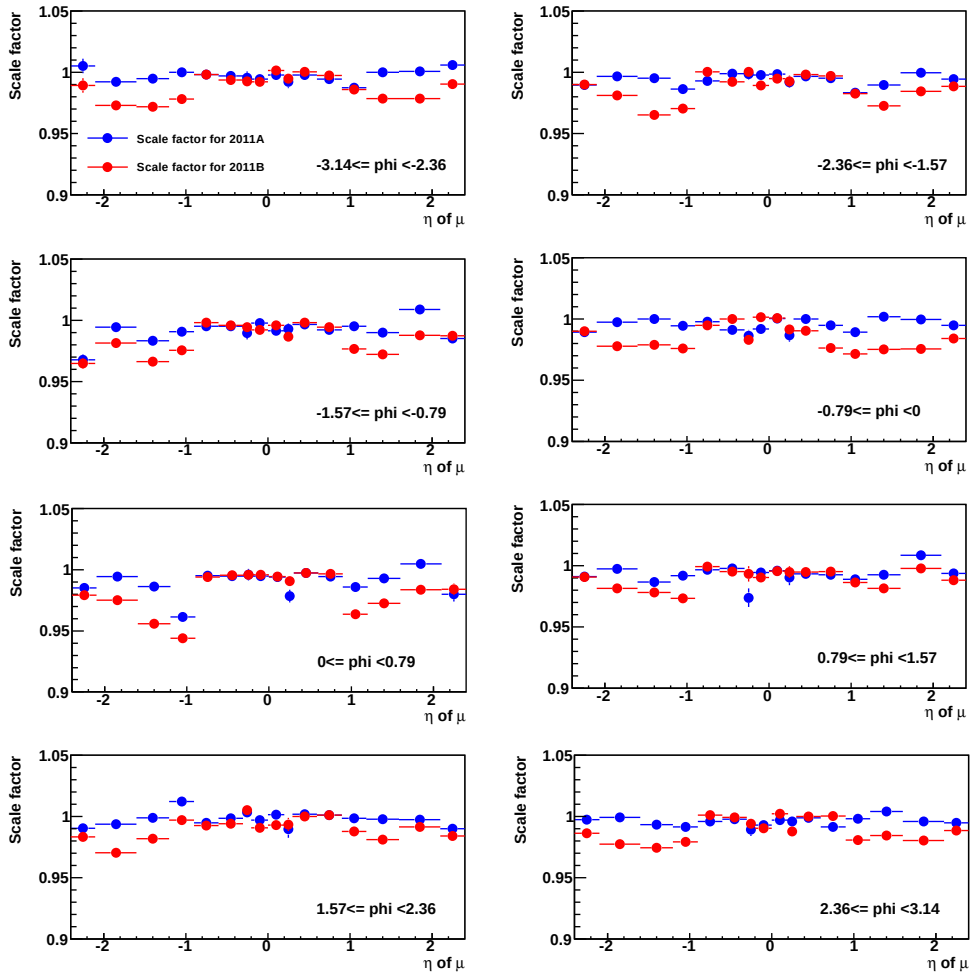

Figure 8: The total (global x ID x Iso) efficiency scale factor (data to MC) as a function of η for each ϕ bin. The blue points are the efficiency for 2011A data, and the red points are for 2011B, and the black points are for MC.

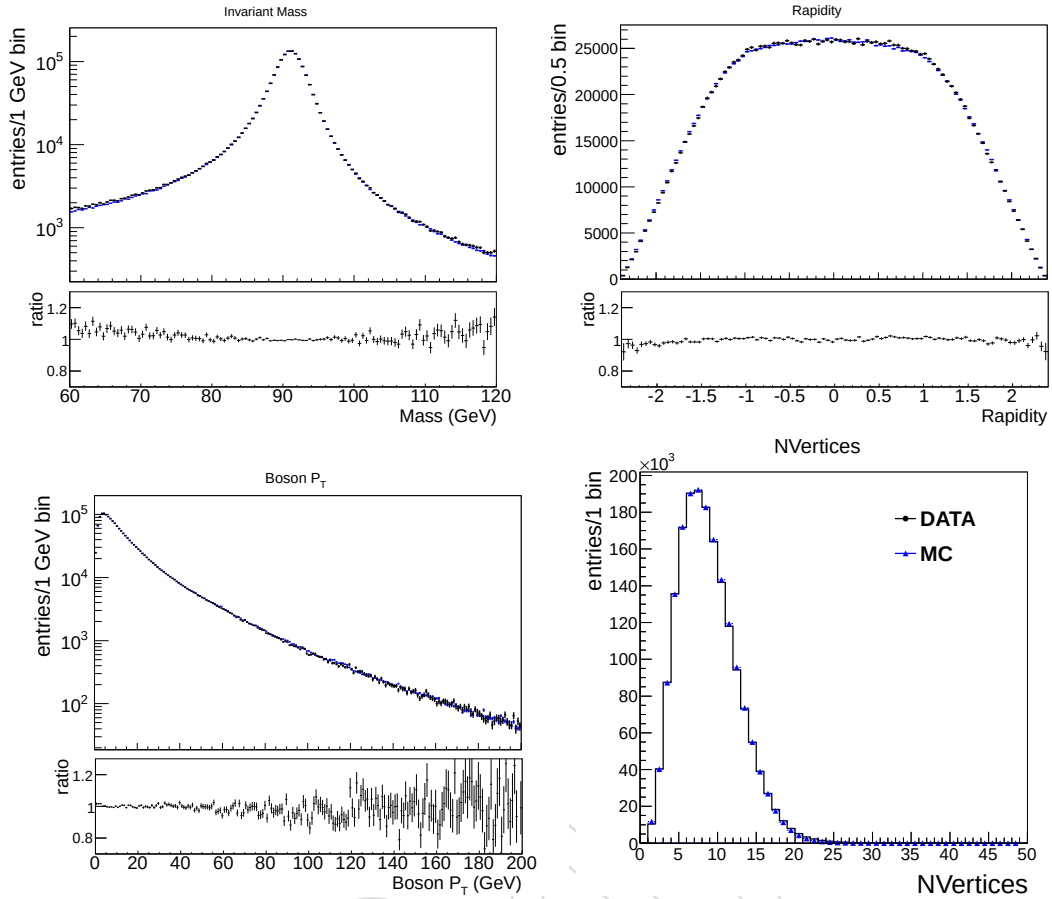

Figure 9: Top Plots: Comparison of the invariant mass (left) and boson rapidity (right) distributions between the data (black) and MC (blue). Bottom plots: Comparison of boson P_T (left) and the number of Z vertices (right) distributions between the data (black) and MC (blue).

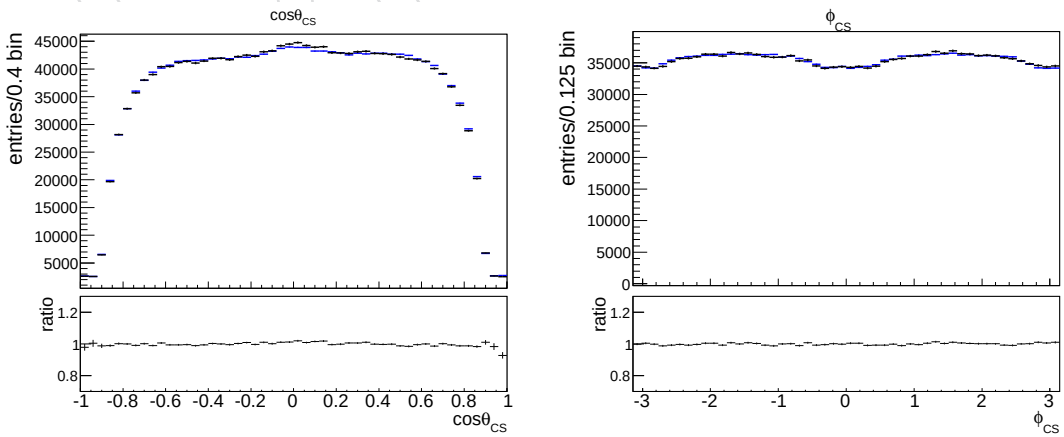

Figure 10: Comparison of the $\cos\theta$ (left) and ϕ (right) distributions in the Collins-Soper frame between the data (black) and MC (blue).

Using MC, we can get the ratio of a background process (such as $t\bar{t}$) to decay to $\mu\mu$ or $e\mu$ in the final state. We assume this ratio to be some constant

$$\frac{t\bar{t} \to \mu\mu}{t\bar{t} \to e\mu} = Constant. \tag{6}$$

This constant should be the same in data as in MC, such that

$$\frac{t\bar{t}_{data} \to \mu\mu}{t\bar{t}_{data} \to e\mu} = Constant = \frac{t\bar{t}_{MC} \to \mu\mu}{t\bar{t}_{MC} \to e\mu}. \tag{7}$$

Rearranging this equation shows that we can estimate the number of $\mu\mu$ background events which come from $t\bar{t}$ events in our sample:

$$t\bar{t}_{data} \to \mu\mu = \frac{t\bar{t}_{MC} \to \mu\mu}{t\bar{t}_{MC} \to e\mu}(t\bar{t}_{data} \to e\mu). \tag{8}$$

We use this $e\mu$ method to estimate all EWK backgrounds. One benefit of using this method is that many systematic divide out when the $e\mu$ to $\mu\mu$ ratio is taken, so that the data-driven method often has smaller total uncertainties than a pure-MC background.

It is not pratical to generate sufficient MC QCD samples to calculate the QCD background using the $e\mu$ method. We exclude QCD MC when we make the same-sign dilepton distributions and assume that the difference between the data and MC distributions comes from the missing QCD events. We have performed MC studies showing that the majority of QCD events which pass our selection cuts come from b-quarks. Assuming all the missing same-sign QCD events come from b-quarks, we can calculate the number of expected opposite-sign $e\mu$ and $\mu\mu$ pairs and add those to the background sample. This method accounts for all EWK and QCD background processes. We show the final MC and data-driven background estimates in Figure 11.

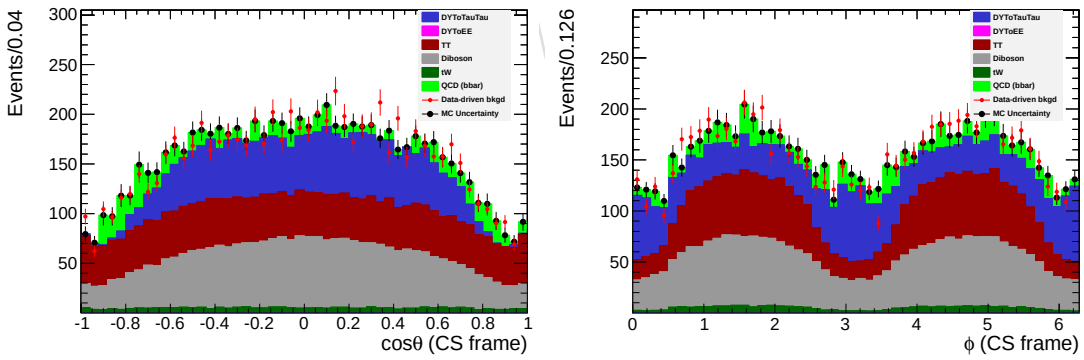

Figure 11: MC and data-driven backgrounds of $\cos\theta$ and ϕ in the Colins-Soper frame.

3.4 Extraction of Angular coefficients

3.4.1 2-dimentional fitting method

We assume that the observed CMS angular distribution factors into the acceptance and the underlying distribution as

$$\frac{d\sigma}{d\Omega} = A(\cos\theta, \phi)s(\cos\theta, \phi) + A(\cos\theta, \phi)b(\cos\theta, \phi) \tag{9}$$

where $A(\cos\theta, \phi)$ is the acceptance, $w(\cos\theta, \phi)$ is the angular distribution containing all angular coefficients ($A_0 - A_7$), and $B(\cos\theta, \phi)$ is the background distribution. We perform a χ^2 fit in each transverse momentum range to extract all eight angular coefficients which give the best overall fit to the observed data distribution. We fit the background distribution $b(\cos\theta, \phi)$ with the general angular distribution expression for a spin-1 particle with an extra $\cos^4\theta$ term.

3.4.2 1-dimentional fitting method

For each transverse momentum range, data and *POWHEG* Monte Carlo simulated events are binned in $\cos\theta$. The Monte Carlo (MC) events are re-weighted to generate the expected experimental distributions for a range of values of A_0 and A_4. A maximum likelihood comparison of the data and Monte Carlo distributions in $\cos\theta$ is used to extract the best values of the angular coefficients A_0 and A_4 that describe the data.

Similarly, for each transverse momentum range, data and Monte Carlo simulated events are also binned in ϕ. A maximum likelihood comparison of the data and Monte Carlo distributions in ϕ is used to extract the best values of the angular coefficients A_2 and A_3 that describe the data.

3.5 Systematic uncertainty

In this section, we summarize the systematic uncertainty sources considered in the measurement. We consider the systematic uncertainty contribution from the efficiency measurement, the muon momentum correction, the background estimation, the pile-up correction, the modeling of Z P_T distribution, QED final state radiation (FSR) modeling, and PDFs.

The muon reconstruction efficiency is estimated using the tag and probe method as a function of η and ϕ and the signal yield is extracted from Z mass fitting method ($60 < M_{\mu^+\mu^-} < 120$ GeV/c^2). This efficiency is also measured using the event counting method in the tight mass window, $80 < M_{\mu^+\mu^-} < 100$ GeV/c^2, to reduce the background contamination. The efficiency deviation between the fitting method vs. the event counting method is assigned as a systematic uncertainty of the efficiency measurement. To assign the systematic uncertainty from the efficiency in the angular coefficients measurement, we smear the efficiency scale factor by 1 sigma of the total error and run toy MC samples varying the efficiency scale factor. The RMS of the deviation from toy MC tests is assigned as a systematic uncertainty for the muon reconstruction efficiency.

For the systematic uncertainty of the muon momentum correction, we also use the same approach used for the systematic uncertainty of the efficiency. The muon momentum correction has its own uncertainty of the measurement and the central value of the muon momentum correction is smeared by 1 sigma of the total error in each toy MC sample. The RMS of the deviation from the central value in the angular coefficients from toy MC tests is assigned as a systematic uncertainty for the muon momentum correction.

The background estimation has $\sim$ 30 % of systematic uncertainty overall. We vary the background with $\pm$ 1 sigma of total error (stat. $\oplus$ syst.) as a function of $\cos\theta_{CS}$ and ϕ_{CS} and estimate the deviation of the angular coefficients. The deviation from the central value is assigned as a systematic uncertainty of the background estimation.

Since MC is generated in low pile-up scenario, the pile-up correction is applied to MC to match to the data. The pile-up distribution measured in the data has $\sim$ 5% level of the systematic uncertainty. Therefore, we vary the pile-up distribution of the data by $\pm$ 5 % and recalculate the pile-up correction of data to MC. This recalculated pile-up correction is applied in MC and ex-

DRAFT

tracted the angular coefficients using this re-weighted MC sample. We compare the difference between the central value and the re-extracted angular coefficients with $\pm$ 5% changes and the deviation is assigned as a systematic uncertainty for the pile-up correction.

Z P_T distribution in POWHEG MC doesn't describe the data well. We derived the Z P_T correction using the data-driven method and the measured correction is applied to MC. This data-driven Z P_T correction is compared with the high order QCD prediction, MadGraph, which is shown in Figure 2. To assign the systematic uncertainty for Z P_T modeling, we measure the angular coefficients with MadGraph Z P_T correction and estimate the deviation of the angular coefficients measured with the data-driven Z P_T correction.

For QED final state radiation (FSR), we rely on POWHEG FSR modeling in the measurement. To estimate the systematic uncertainty of FSR modeling, we applied FSR reweighing factor developed using a parton-shower approach (Pythia) and assign the difference with FSR reweighing in the angular coefficients measurement as a systematic uncertainty.

POWHEG MC sample uses CT10 PDFs as a default. To assign the systematic uncertainty of PDFs modeling, we consider CT10, MSTW2008nlo, and NNPDF2.0 PDFs set with 68% CL variation. The deviation from various PDFs weighting is considered to assign the systematic uncertainty of PDFs.

3.6 Result

The results for A_0, A_2, A_3, and A_4 are shown in Figure 12 and 13 with full statisical and systematic uncertainties. A breakdown of the full systematics is shown in Tables 2-9 for 2D fitting result and Tables 10-17 for 1D fitting result. Results are dominated by statistical uncertainty with PDF uncertainty being the next largest contributor. Results from the two different fitting methods have good agreement with each other. A_0 and A_2 tend to increase with Z P_T as expected within the predicted limits for $q\bar{q}$ and qg production though A_2 values deviate from POWHEG predictions as Z P_T increases, most notably in the higher rapidity bin. We are investigating this effect to understand if there is a need to adjust the fitting procedure for high Z P_T or if we could be observing effects of higher-order QCD processes. The values for A_3 are consistent with zero as predicted by theory. Values for A_4 are also consistent between the two methods and consistent with POWHEG predictions within uncertainties.

Results of the fit for A_1 are shown in Figure 14 for the 2D fitting method only since the 1D fitting method cannot observe A_1. There is generally good agreement between the fit results with POWHEG, with better agreement at lower Zy. Results for A_5, A_6, and A_7 are not shown here but are consistent with zero as predicted by theory.

References

[1] E. Mirkes and J. Ohnemus *Phys. Rev. D* **50, 51** (1994, 1995) 5692, 4891.

[2] J. C. Collins and D. E. Soper *Phys. Rev. D* **16** (1977) 2219.

[3] "The coordinates in the laboratory frame are (θ,ϕ,z), where θ is the polar angle relative to the direction of one of the proton beams(the $+z$ axis), and ϕ the azimuth. The pseudorapidity is $\eta = -ln\ tan(\theta/2)$. For an $\mu^+ + \mu^-$ pair $P_T = Psin\theta$, $E_T = Esin\theta$, and $y = \frac{1}{2}ln\frac{E+P_z}{E-P_z}$, where P and P_z are the magnitude and z component of the momentum, and E is the energy of the $\mu^+ + \mu^-$ pair",.

[4] J. C. Collins *Phys. Rev. Lett.* **42** (1979) 291.

DRAFT

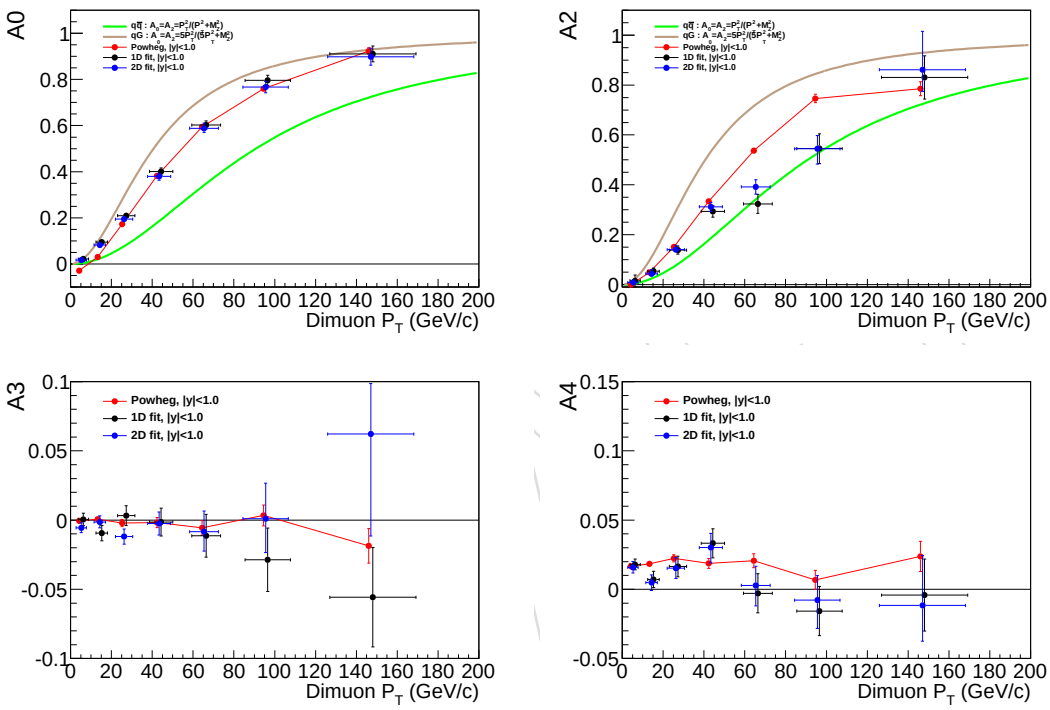

Figure 12: Comparison of the CMS measured values of A_0, A_2, A_3 and A_4 (shown with full statistical and systematic uncertainties) for $|Zy| < 1.0$ with the 1D and 2D fitting methods and POWHEG predictions. Results of the two different methods have agreement within uncertainties. Results disagree with A_2 POWHEG predictions as Z_PT increases.

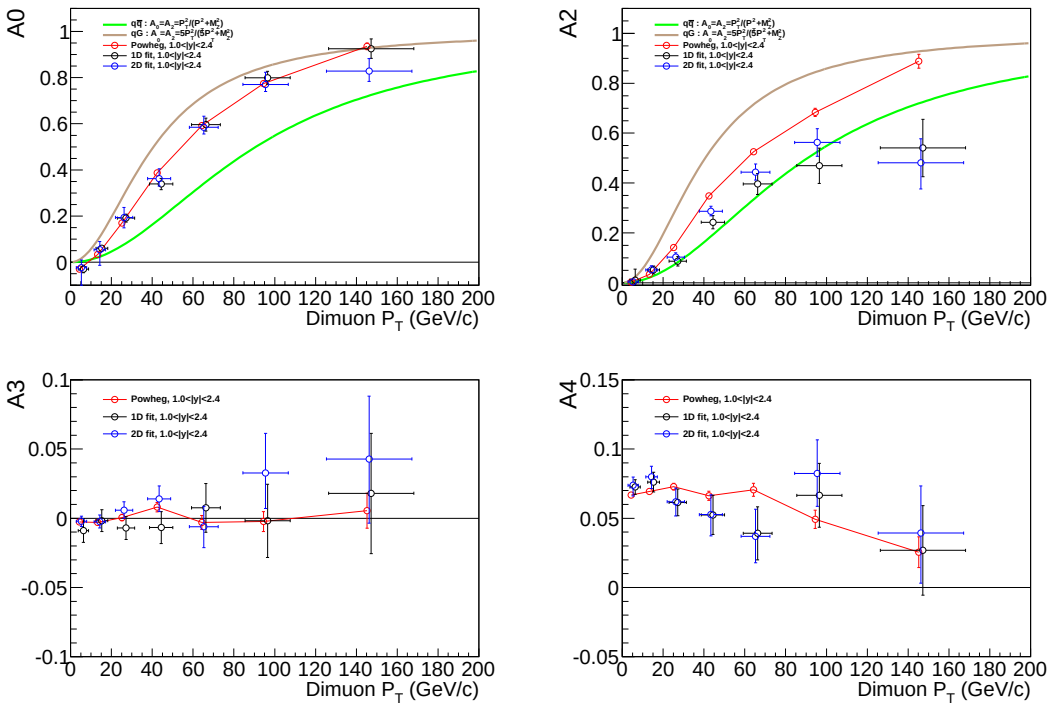

Figure 13: Comparison of the CMS measured values of A_0, A_2, A_3 and A_4 (shown with full statistical and systematic uncertainties) for $1.0 < |Zy| < 2.4$ with the 1D and 2D fitting methods and POWHEG predictions. Results of the two different methods have agreement within uncertainties. Results disagree with A_2 POWHEG predictions as Z_PT increases.

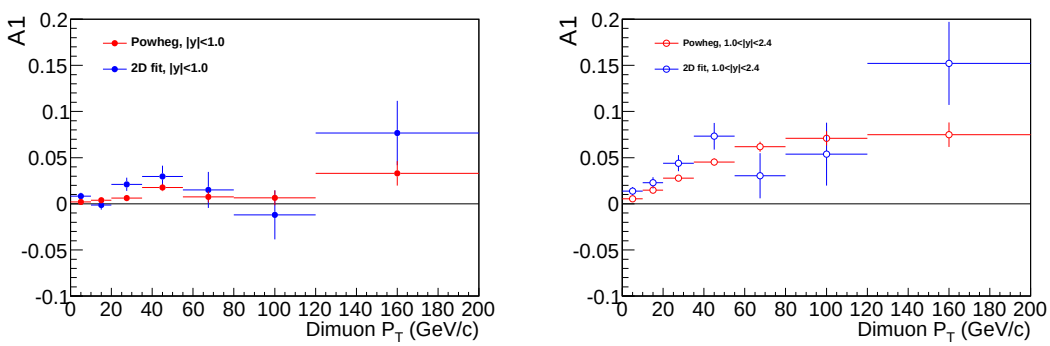

Figure 14: Comparison of the CMS measured values of A_1 (shown with full statistical and systematic uncertainties) for $|Zy|$ <1. (left) and $1.0 < |Zy| < 2.4$ (right) between the 1D fitting method and POWHEG predictions.

γ^*/ZP_T; $0.0 \leq \lvert Y \rvert < 1.0$	0–10	10–20	20–35	35–55	55–80	80–120	120–200
A0 Central Value	0.0173	0.0827	0.1947	0.3799	0.5883	0.7340	0.9026
Stat. Uncert.	0.0047	0.0074	0.0095	0.0133	0.0169	0.0229	0.0360
PU Syst.	$\pm^{0.0006}_{0.0071}$	$\pm^{0.0003}_{0.0065}$	$\pm^{0.0005}_{0.0076}$	$\pm^{0.0002}_{0.0095}$	$\pm^{0.0009}_{0.0046}$	$\pm^{0.0038}_{0.0007}$	$\pm^{0.0005}_{0.0019}$
Mom. Corr. Syst	0.0007	0.0010	0.0010	0.0010	0.0020	0.0049	0.0027
TnP Syst	0.0020	0.0020	0.0018	0.0020	0.0023	0.0051	0.0021
ZP_T Syst	0.0009	0.0009	0.0007	0.0017	0.0043	0.0060	0.0028
Finite MC	0.0016	0.0007	0.0007	0.0006	0.0005	0.0005	0.0005
MSTW PDF Syst	$\pm^{0.0000}_{0.0014}$	$\pm^{0.0023}_{0.0002}$	$\pm^{0.0000}_{0.0010}$	$\pm^{0.0000}_{0.0002}$	$\pm^{0.0038}_{0.0001}$	$\pm^{0.0002}_{0.0002}$	$\pm^{0.0004}_{0.0005}$
nnpdf PDF Syst	$\pm^{0.0001}_{0.0059}$	$\pm^{0.0055}_{0.0007}$	$\pm^{0.0024}_{0.0018}$	$\pm^{0.0015}_{0.0005}$	$\pm^{0.0138}_{0.0000}$	$\pm^{0.0036}_{0.0003}$	$\pm^{0.0054}_{0.0012}$
Bkgd Syst	$\pm^{0.0007}_{0.0007}$	$\pm^{0.0011}_{0.0011}$	$\pm^{0.0011}_{0.0012}$	$\pm^{0.0002}_{0.0001}$	$\pm^{0.0017}_{0.0016}$	$\pm^{0.0020}_{0.0021}$	$\pm^{0.0001}_{0.0003}$
FSR Syst	0.0001	0.0010	0.0014	0.0003	0.0002	0.0002	0.0000

Table 2: A_0 central value and uncertainties for $|y| < 1.0$ from 2D fit result.

γ^*/ZP_T; $1.0 \leq \lvert Y \rvert < 2.4$	0–10	10–20	20–35	35–55	55–80	80–120	120–200
A0 Central Value	-0.0234	0.0538	0.1938	0.3623	0.5845	0.7169	0.6990
Stat. Uncert.	0.0069	0.0101	0.0139	0.0200	0.0242	0.0285	0.0452
PU Syst.	$\pm^{0.0002}_{0.0002}$	$\pm^{0.0005}_{0.0007}$	$\pm^{0.0003}_{0.0064}$	$\pm^{0.0024}_{0.0012}$	$\pm^{0.0010}_{0.0009}$	$\pm^{0.0007}_{0.0026}$	$\pm^{0.0036}_{0.0024}$
Mom. Corr. Syst	0.0004	0.0007	0.0008	0.0020	0.0017	0.0024	0.0025
TnP Syst	0.0028	0.0028	0.0029	0.0034	0.0026	0.0028	0.0026
ZP_T Syst	0.0004	0.0009	0.0013	0.0025	0.0051	0.0071	0.0065
Finite MC	0.0014	0.0012	0.0009	0.0009	0.0007	0.0006	0.0015
MSTW PDF Syst	$\pm^{0.0032}_{0.0263}$	$\pm^{0.0027}_{0.0221}$	$\pm^{0.0025}_{0.0105}$	$\pm^{0.0058}_{0.0029}$	$\pm^{0.0142}_{0.0002}$	$\pm^{0.0261}_{0.0002}$	$\pm^{0.0168}_{0.0002}$
nnpdf PDF Syst	$\pm^{0.0316}_{0.0763}$	$\pm^{0.0342}_{0.0626}$	$\pm^{0.0410}_{0.0408}$	$\pm^{0.0373}_{0.0242}$	$\pm^{0.0389}_{0.0130}$	$\pm^{0.0353}_{0.0057}$	$\pm^{0.0258}_{0.0032}$
Bkgd Syst	$\pm^{0.0003}_{0.0003}$	$\pm^{0.0002}_{0.0003}$	$\pm^{0.0002}_{0.0003}$	$\pm^{0.0011}_{0.0010}$	$\pm^{0.0037}_{0.0036}$	$\pm^{0.0063}_{0.0060}$	$\pm^{0.0002}_{0.0005}$
FSR Syst	0.0001	0.0004	0.0012	0.0003	0.0002	0.0001	0.0002

Table 3: A_0 central value and uncertainties for $1.0 \leq |y| < 2.4$ from 2D fit result.

[5] D. Boer and W. Vogelsang *Phys. Rev. D.* **74** (2006) 014004.

[6] E. L. Berger, J.-W. Qiu, and R. A. Rodriguez-Pedraza *Phys. Lett. B.* **656** (2007) 74.

[7] A. Bodek *Eur.Phys.J. C* **67** (2010) 321.

[8] L. Y. Z. et al. *Phys. Rev. Lett.* **99** (2007) 082301.

[9] J. Lindfors *Physica Scripta* **20** (1979) 19.

[10] J. H. W. S. Bodek, A. van Dyne and A. Strelnikov *Eur. Phys. J. C* **72** (2012) 72.

[11] CMS Collaboration Technical Report CMS AN 2012/298, (2012).

[12] CMS Collaboration Technical Report CMS AN 2012/062, (2012).

DRAFT

γ^*/ZP_T; $0.0 \leq \lvert Y \rvert < 1.0$	0–10	10–20	20–35	35–55	55–80	80–120	120–200
A2 Central Value	0.0085	0.0434	0.1401	0.3121	0.3920	0.5032	0.9979
Stat. Uncert.	0.0062	0.0083	0.0110	0.0167	0.0276	0.0501	0.0782
PU Syst.	$\pm^{0.0002}_{0.0003}$	$\pm^{0.0002}_{0.0027}$	$\pm^{0.0003}_{0.0022}$	$\pm^{0.0006}_{0.0041}$	$\pm^{0.0019}_{0.0054}$	$\pm^{0.0054}_{0.0041}$	$\pm^{0.0067}_{0.0237}$
Mom. Corr. Syst	0.0006	0.0006	0.0010	0.0008	0.0026	0.0101	0.0088
TnP Syst	0.0006	0.0002	0.0004	0.0011	0.0006	0.0093	0.0088
ZP_T Syst	0.0058	0.0024	0.0020	0.0018	0.0047	0.0107	0.0106
Finite MC	0.0019	0.0008	0.0007	0.0007	0.0009	0.0011	0.0011
MSTW PDF Syst	$\pm^{0.0001}_{0.0010}$	$\pm^{0.0010}_{0.0002}$	$\pm^{0.0020}_{0.0000}$	$\pm^{0.0001}_{0.0026}$	$\pm^{0.0019}_{0.0002}$	$\pm^{0.0000}_{0.0054}$	$\pm^{0.0777}_{0.0000}$
nnpdf PDF Syst	$\pm^{0.0036}_{0.0009}$	$\pm^{0.0133}_{0.0001}$	$\pm^{0.0131}_{0.0000}$	$\pm^{0.0002}_{0.0060}$	$\pm^{0.0054}_{0.0025}$	$\pm^{0.0000}_{0.0287}$	$\pm^{0.1022}_{0.0001}$
Bkgd Syst	$\pm^{0.0002}_{0.0002}$	$\pm^{0.0012}_{0.0012}$	$\pm^{0.0003}_{0.0002}$	$\pm^{0.0012}_{0.0012}$	$\pm^{0.0019}_{0.0019}$	$\pm^{0.0002}_{0.0000}$	$\pm^{0.0035}_{0.0032}$
FSR Syst	0.0005	0.0016	0.0012	0.0003	0.0007	0.0007	0.0002

Table 4: A_2 central value and uncertainties for $|y| < 1.0$ from 2D fit result.

γ^*/ZP_T; $1.0 \leq \lvert Y \rvert < 2.4$	0–10	10–20	20–35	35–55	55–80	80–120	120–200
A2 Central Value	0.0041	0.0516	0.1026	0.2868	0.4432	0.4973	0.5788
Stat. Uncert.	0.0063	0.0085	0.0115	0.0175	0.0287	0.0516	0.0895
PU Syst.	$\pm^{0.0003}_{0.0005}$	$\pm^{0.0004}_{0.0007}$	$\pm^{0.0010}_{0.0014}$	$\pm^{0.0010}_{0.0023}$	$\pm^{0.0006}_{0.0088}$	$\pm^{0.0000}_{0.0137}$	$\pm^{0.0059}_{0.0240}$
Mom. Corr. Syst	0.0003	0.0006	0.0008	0.0013	0.0031	0.0069	0.0083
TnP Syst	0.0001	0.0008	0.0005	0.0008	0.0036	0.0058	0.0075
ZP_T Syst	0.0091	0.0033	0.0025	0.0019	0.0066	0.0114	0.0116
Finite MC	0.0012	0.0009	0.0008	0.0009	0.0009	0.0012	0.0087
MSTW PDF Syst	$\pm^{0.0002}_{0.0014}$	$\pm^{0.0005}_{0.0014}$	$\pm^{0.0003}_{0.0010}$	$\pm^{0.0018}_{0.0000}$	$\pm^{0.0030}_{0.0001}$	$\pm^{0.0023}_{0.0004}$	$\pm^{0.0007}_{0.0062}$
nnpdf PDF Syst	$\pm^{0.0038}_{0.0022}$	$\pm^{0.0135}_{0.0020}$	$\pm^{0.0124}_{0.0000}$	$\pm^{0.0082}_{0.0002}$	$\pm^{0.0142}_{0.0000}$	$\pm^{0.0140}_{0.0036}$	$\pm^{0.0154}_{0.0375}$
Bkgd Syst	$\pm^{0.0002}_{0.0002}$	$\pm^{0.0010}_{0.0010}$	$\pm^{0.0005}_{0.0006}$	$\pm^{0.0009}_{0.0010}$	$\pm^{0.0028}_{0.0029}$	$\pm^{0.0031}_{0.0027}$	$\pm^{0.0003}_{0.0003}$
FSR Syst	0.0004	0.0016	0.0014	0.0001	0.0008	0.0008	0.0004

Table 5: A_2 central value and uncertainties for $1.0 \leq |y| < 2.4$ from 2D fit result.

DRAFT

γ^*/ZP_T; $0.0 \leq \lvert Y \rvert < 1.0$	0–10	10–20	20–35	35–55	55–80	80–120	120–200
A3 Central Value	-0.0056	-0.0014	-0.0119	-0.0025	-0.0085	0.0068	0.0159
Stat. Uncert.	0.0029	0.0038	0.0052	0.0082	0.0136	0.0225	0.0359
PU Syst.	$\pm^{0.0001}_{0.0003}$	$\pm^{0.0002}_{0.0004}$	$\pm^{0.0005}_{0.0008}$	$\pm^{0.0003}_{0.0004}$	$\pm^{0.0008}_{0.0004}$	$\pm^{0.0006}_{0.0054}$	$\pm^{0.0010}_{0.0074}$
Mom. Corr. Syst	0.0020	0.0015	0.0012	0.0011	0.0022	0.0038	0.0044
TnP Syst	0.0002	0.0002	0.0001	0.0002	0.0017	0.0045	0.0038
ZP_T Syst	0.0002	0.0002	0.0001	0.0002	0.0017	0.0043	0.0038
Finite MC	0.0009	0.0004	0.0004	0.0004	0.0004	0.0005	0.0005
MSTW PDF Syst	$\pm^{0.0000}_{0.0000}$	$\pm^{0.0008}_{0.0000}$	$\pm^{0.0001}_{0.0000}$	$\pm^{0.0004}_{0.0001}$	$\pm^{0.0034}_{0.0001}$	$\pm^{0.0014}_{0.0001}$	$\pm^{0.0000}_{0.0280}$
nnpdf PDF Syst	$\pm^{0.0002}_{0.0002}$	$\pm^{0.0017}_{0.0003}$	$\pm^{0.0005}_{0.0003}$	$\pm^{0.0002}_{0.0014}$	$\pm^{0.0041}_{0.0002}$	$\pm^{0.0095}_{0.0000}$	$\pm^{0.0000}_{0.0571}$
Bkgd Syst	$\pm^{0.0000}_{0.0000}$	$\pm^{0.0000}_{0.0000}$	$\pm^{0.0000}_{0.0000}$	$\pm^{0.0001}_{0.0001}$	$\pm^{0.0003}_{0.0002}$	$\pm^{0.0000}_{0.0001}$	$\pm^{0.0010}_{0.0009}$
FSR Syst	0.0000	0.0000	0.0000	0.0000	0.0000	0.0002	0.0001

Table 6: A_3 central value and uncertainties for $|y| < 1.0$ from 2D fit result.

γ^*/ZP_T; $1.0 \leq \lvert Y \rvert < 2.4$	0–10	10–20	20–35	35–55	55–80	80–120	120–200
A3 Central Value	-0.0022	-0.0025	0.0057	0.0140	-0.0061	0.0276	0.0420
Stat. Uncert.	0.0029	0.0040	0.0055	0.0087	0.0146	0.0244	0.0409
PU Syst.	$\pm^{0.0004}_{0.0011}$	$\pm^{0.0003}_{0.0011}$	$\pm^{0.0003}_{0.0002}$	$\pm^{0.0008}_{0.0016}$	$\pm^{0.0001}_{0.0006}$	$\pm^{0.0005}_{0.0028}$	$\pm^{0.0017}_{0.0035}$
Mom. Corr. Syst	0.0020	0.0017	0.0014	0.0012	0.0015	0.0034	0.0095
TnP Syst	0.0001	0.0006	0.0004	0.0005	0.0008	0.0039	0.0105
ZP_T Syst	0.0001	0.0006	0.0004	0.0005	0.0009	0.0036	0.0106
Finite MC	0.0005	0.0004	0.0004	0.0004	0.0005	0.0005	0.0038
MSTW PDF Syst	$\pm^{0.0000}_{0.0004}$	$\pm^{0.0000}_{0.0003}$	$\pm^{0.0004}_{0.0000}$	$\pm^{0.0010}_{0.0000}$	$\pm^{0.0003}_{0.0001}$	$\pm^{0.0070}_{0.0002}$	$\pm^{0.0005}_{0.0005}$
nnpdf PDF Syst	$\pm^{0.0007}_{0.0005}$	$\pm^{0.0020}_{0.0000}$	$\pm^{0.0023}_{0.0005}$	$\pm^{0.0024}_{0.0010}$	$\pm^{0.0007}_{0.0038}$	$\pm^{0.0104}_{0.0000}$	$\pm^{0.0050}_{0.0092}$
Bkgd Syst	$\pm^{0.0000}_{0.0000}$	$\pm^{0.0001}_{0.0001}$	$\pm^{0.0000}_{0.0001}$	$\pm^{0.0002}_{0.0003}$	$\pm^{0.0002}_{0.0002}$	$\pm^{0.0001}_{0.0001}$	$\pm^{0.0007}_{0.0007}$
FSR Syst	0.0000	0.0000	0.0000	0.0000	0.0000	0.0001	0.0002

Table 7: A_3 central value and uncertainties for $1.0 \leq |y| < 2.4$ from 2D fit result.

DRAFT

γ^*/ZP_T; $0.0 \leq \lvert Y \rvert < 1.0$	0–10	10–20	20–35	35–55	55–80	80–120	120–200
A4 Central Value	0.0158	0.0048	0.0152	0.0301	0.0028	-0.0068	-0.0141
Stat. Uncert.	0.0039	0.0054	0.0072	0.0102	0.0138	0.0181	0.0250
PU Syst.	$\pm^{0.0002}_{0.0001}$	$\pm^{0.0002}_{0.0011}$	$\pm^{0.0002}_{0.0016}$	$\pm^{0.0008}_{0.0004}$	$\pm^{0.0003}_{0.0027}$	$\pm^{0.0007}_{0.0007}$	$\pm^{0.0015}_{0.0057}$
Mom. Corr. Syst	0.0002	0.0003	0.0003	0.0006	0.0008	0.0008	0.0031
TnP Syst	0.0001	0.0002	0.0001	0.0005	0.0007	0.0002	0.0022
ZP_T Syst	0.0001	0.0002	0.0001	0.0005	0.0007	0.0003	0.0022
Finite MC	0.0011	0.0005	0.0005	0.0004	0.0004	0.0004	0.0003
MSTW PDF Syst	$\pm^{0.0006}_{0.0001}$	$\pm^{0.0006}_{0.0001}$	$\pm^{0.0015}_{0.0001}$	$\pm^{0.0000}_{0.0004}$	$\pm^{0.0000}_{0.0006}$	$\pm^{0.0000}_{0.0029}$	$\pm^{0.0130}_{0.0006}$
nnpdf PDF Syst	$\pm^{0.0011}_{0.0005}$	$\pm^{0.0008}_{0.0012}$	$\pm^{0.0020}_{0.0001}$	$\pm^{0.0002}_{0.0041}$	$\pm^{0.0000}_{0.0041}$	$\pm^{0.0000}_{0.0097}$	$\pm^{0.0223}_{0.0013}$
Bkgd Syst	$\pm^{0.0000}_{0.0000}$	$\pm^{0.0001}_{0.0001}$	$\pm^{0.0000}_{0.0000}$	$\pm^{0.0001}_{0.0001}$	$\pm^{0.0002}_{0.0002}$	$\pm^{0.0001}_{0.0000}$	$\pm^{0.0003}_{0.0003}$
FSR Syst	0.0000	0.0000	0.0000	0.0001	0.0000	0.0000	0.0000

Table 8: A_4 central value and uncertainties for $|y| < 1.0$ from 2D fit result.

γ^*/ZP_T; $1.0 \leq \lvert Y \rvert < 2.4$	0–10	10–20	20–35	35–55	55–80	80–120	120–200
A4 Central Value	0.0738	0.0799	0.0619	0.0526	0.0370	0.0768	0.0030
Stat. Uncert.	0.0053	0.0071	0.0096	0.0139	0.0189	0.0233	0.0334
PU Syst.	$\pm^{0.0004}_{0.0008}$	$\pm^{0.0003}_{0.0017}$	$\pm^{0.0001}_{0.0010}$	$\pm^{0.0029}_{0.0034}$	$\pm^{0.0007}_{0.0013}$	$\pm^{0.0024}_{0.0003}$	$\pm^{0.0027}_{0.0048}$
Mom. Corr. Syst	0.0003	0.0004	0.0010	0.0010	0.0008	0.0024	0.0052
TnP Syst	0.0003	0.0004	0.0008	0.0005	0.0007	0.0029	0.0034
ZP_T Syst	0.0003	0.0004	0.0008	0.0006	0.0008	0.0032	0.0037
Finite MC	0.0010	0.0007	0.0007	0.0006	0.0006	0.0005	0.0021
MSTW PDF Syst	$\pm^{0.0000}_{0.0048}$	$\pm^{0.0000}_{0.0033}$	$\pm^{0.0002}_{0.0005}$	$\pm^{0.0000}_{0.0039}$	$\pm^{0.0000}_{0.0019}$	$\pm^{0.0001}_{0.0047}$	$\pm^{0.0032}_{0.0001}$
nnpdf PDF Syst	$\pm^{0.0023}_{0.0024}$	$\pm^{0.0028}_{0.0020}$	$\pm^{0.0021}_{0.0034}$	$\pm^{0.0015}_{0.0034}$	$\pm^{0.0044}_{0.0006}$	$\pm^{0.0066}_{0.0027}$	$\pm^{0.0074}_{0.0146}$
Bkgd Syst	$\pm^{0.0000}_{0.0000}$	$\pm^{0.0002}_{0.0002}$	$\pm^{0.0001}_{0.0001}$	$\pm^{0.0001}_{0.0001}$	$\pm^{0.0005}_{0.0005}$	$\pm^{0.0011}_{0.0011}$	$\pm^{0.0004}_{0.0004}$
FSR Syst	0.0000	0.0000	0.0001	0.0000	0.0001	0.0000	0.0002

Table 9: A_4 central value and uncertainties for $1.0 \leq |y| < 2.4$ from 2D fit result.

DRAFT

γ^*/ZP_T; $0.0 \leq \lvert Y \rvert < 1.0$	0–10	10–20	20–35	35–55	55–80	80–120	120–200
A0 Central Value	0.0218	0.0953	0.2095	0.4008	0.6026	0.7960	0.9106
Stat. Uncert.	0.0055	0.0080	0.0111	0.0144	0.0169	0.0217	0.0346
Syst. Uncert.	$\pm^{0.0030}_{0.0031}$	$\pm^{0.0038}_{0.0039}$	$\pm^{0.0049}_{0.0049}$	$\pm^{0.0051}_{0.0050}$	$\pm^{0.0052}_{0.0050}$	$\pm^{0.0044}_{0.0046}$	$\pm^{0.0027}_{0.0028}$
PU Syst	$\pm^{0.0006}_{0.0006}$	$\pm^{0.0000}_{0.0003}$	$\pm^{0.0004}_{0.0005}$	$\pm^{0.0002}_{0.0002}$	$\pm^{0.0006}_{0.0005}$	$\pm^{0.0031}_{0.0035}$	$\pm^{0.0008}_{0.0003}$
Mom. Corr. Syst	0.0017	0.0029	0.0030	0.0022	0.0018	0.0017	0.0020
TnP Syst	0.0015	0.0015	0.0015	0.0013	0.0012	0.0009	0.0009
Z P_T Syst	0.0017	0.0003	0.0023	0.0003	0.0002	0.0004	0.0009
Bkgd Syst	$\pm^{0.0010}_{0.0011}$	$\pm^{0.0020}_{0.0021}$	$\pm^{0.0027}_{0.0026}$	$\pm^{0.0044}_{0.0043}$	$\pm^{0.0046}_{0.0045}$	$\pm^{0.0023}_{0.0023}$	$\pm^{0.0011}_{0.0014}$

Table 10: A_0 central value and uncertainties for $|y| < 1.0$ from 1D fit result.

γ^*/ZP_T; $1.0 \leq \lvert Y \rvert < 2.4$	0–10	10–20	20–35	35–55	55–80	80–120	120–200
A0 Central Value	-0.0296	0.0602	0.1913	0.3390	0.5960	0.7995	0.9255
Stat. Uncert.	0.0084	0.0118	0.0164	0.0230	0.0265	0.0279	0.0411
Syst. Uncert.	$\pm^{0.0136}_{0.0136}$	$\pm^{0.0051}_{0.0051}$	$\pm^{0.0055}_{0.0055}$	$\pm^{0.0075}_{0.0069}$	$\pm^{0.0090}_{0.0085}$	$\pm^{0.0047}_{0.0045}$	$\pm^{0.0106}_{0.0103}$
PU Syst	$\pm^{0.0002}_{0.0001}$	$\pm^{0.0003}_{0.0004}$	$\pm^{0.0000}_{0.0002}$	$\pm^{0.0026}_{0.0019}$	$\pm^{0.0007}_{0.0004}$	$\pm^{0.0009}_{0.0005}$	$\pm^{0.0039}_{0.0029}$
Mom. Corr. Syst	0.0005	0.0013	0.0011	0.0017	0.0024	0.0024	0.0059
TnP Syst	0.0035	0.0036	0.0036	0.0035	0.0028	0.0023	0.0016
Z P_T Syst	0.0130	0.0004	0.0023	0.0002	0.0001	0.0007	0.0076
Bkgd Syst	$\pm^{0.0012}_{0.0012}$	$\pm^{0.0034}_{0.0034}$	$\pm^{0.0033}_{0.0032}$	$\pm^{0.0058}_{0.0054}$	$\pm^{0.0081}_{0.0077}$	$\pm^{0.0031}_{0.0029}$	$\pm^{0.0014}_{0.0015}$

Table 11: A_0 central value and uncertainties for $1.0 \leq |y| < 2.4$ from 1D fit result.

γ^*/ZP_T; $0.0 \leq \lvert Y \rvert < 1.0$	0–10	10–20	20–35	35–55	55–80	80–120	120–200
A2 Central Value	0.0155	0.0534	0.1382	0.2935	0.3237	0.5451	0.8308
Stat. Uncert.	0.0093	0.0120	0.0154	0.0224	0.0361	0.0579	0.0848
Syst. Uncert.	$\pm^{0.0213}_{0.0213}$	$\pm^{0.0045}_{0.0045}$	$\pm^{0.0050}_{0.0050}$	$\pm^{0.0045}_{0.0045}$	$\pm^{0.0106}_{0.0108}$	$\pm^{0.0140}_{0.0155}$	$\pm^{0.0156}_{0.0197}$
PU Syst	$\pm^{0.0006}_{0.0006}$	$\pm^{0.0002}_{0.0002}$	$\pm^{0.0004}_{0.0003}$	$\pm^{0.0003}_{0.0001}$	$\pm^{0.0013}_{0.0010}$	$\pm^{0.0028}_{0.0049}$	$\pm^{0.0050}_{0.0095}$
Mom. Corr. Syst	0.0075	0.0013	0.0024	0.0023	0.0064	0.0090	0.0038
TnP Syst	0.0001	0.0002	0.0004	0.0007	0.0005	0.0008	0.0009
Z P_T Syst	0.0199	-0.0042	-0.0043	-0.0011	-0.0025	0.0011	-0.0038
Bkgd Syst	$\pm^{0.0002}_{0.0002}$	$\pm^{0.0008}_{0.0008}$	$\pm^{0.0003}_{0.0003}$	$\pm^{0.0036}_{0.0037}$	$\pm^{0.0080}_{0.0083}$	$\pm^{0.0102}_{0.0115}$	$\pm^{0.0137}_{0.0163}$

Table 12: A_2 central value and uncertainties for $|y| < 1.0$ from 1D fit result.

γ^*/ZP_T; $1.0 \leq \lvert Y \rvert < 2.4$	0–10	10–20	20–35	35–55	55–80	80–120	120–200
A2 Central Value	0.0107	0.0516	0.0869	0.2428	0.3961	0.4697	0.5411
Stat. Uncert.	0.0120	0.0140	0.0176	0.0251	0.0397	0.0672	0.1070
Syst. Uncert.	$\pm^{0.0422}_{0.0422}$	$\pm^{0.0073}_{0.0073}$	$\pm^{0.0076}_{0.0076}$	$\pm^{0.0079}_{0.0081}$	$\pm^{0.0138}_{0.0144}$	$\pm^{0.0215}_{0.0234}$	$\pm^{0.0391}_{0.0451}$
PU Syst	$\pm^{0.0008}_{0.0008}$	$\pm^{0.0011}_{0.0009}$	$\pm^{0.0012}_{0.0007}$	$\pm^{0.0012}_{0.0016}$	$\pm^{0.0001}_{0.0001}$	$\pm^{0.0014}_{0.0017}$	$\pm^{0.0050}_{0.0003}$
Mom. Corr. Syst	0.0007	0.0018	0.0023	0.0026	0.0048	0.0060	0.0000
TnP Syst	0.0001	0.0002	0.0005	0.0008	0.0010	0.0008	0.0016
Z P_T Syst	0.0422	0.0070	0.0071	0.0012	0.0035	0.0024	0.0044
Bkgd Syst	$\pm^{0.0006}_{0.0006}$	$\pm^{0.0007}_{0.0007}$	$\pm^{0.0008}_{0.0009}$	$\pm^{0.0072}_{0.0074}$	$\pm^{0.0125}_{0.0131}$	$\pm^{0.0204}_{0.0224}$	$\pm^{0.0385}_{0.0448}$

Table 13: A_2 central value and uncertainties for $1.0 \leq |y| < 2.4$ from 1D fit result.

DRAFT

γ^*/ZP_T; $0.0 \leq \lvert Y \rvert < 1.0$	0–10	10–20	20–35	35–55	55–80	80–120	120–200
A3 Central Value	0.0005	-0.0094	0.0032	-0.0014	-0.0114	-0.0287	-0.0558
Stat. Uncert.	0.0039	0.0052	0.0067	0.0100	0.0152	0.0228	0.0352
Syst. Uncert.	$\pm^{0.0023}_{0.0022}$	$\pm^{0.0020}_{0.0021}$	$\pm^{0.0021}_{0.0021}$	$\pm^{0.0014}_{0.0014}$	$\pm^{0.0018}_{0.0021}$	$\pm^{0.0029}_{0.0029}$	$\pm^{0.0069}_{0.0068}$
PU Syst	$\pm^{0.0003}_{0.0003}$	$\pm^{0.0001}_{0.0003}$	$\pm^{0.0008}_{0.0007}$	$\pm^{0.0000}_{0.0002}$	$\pm^{0.0005}_{0.0010}$	$\pm^{0.0006}_{0.0008}$	$\pm^{0.0021}_{0.0015}$
Mom. Corr. Syst	0.0022	0.0020	0.0020	0.0014	0.0016	0.0025	0.0061
TnP Syst	0.0001	0.0001	0.0001	0.0001	0.0002	0.0001	0.0004
Z P_T Syst	0.0000	0.0001	0.0001	-0.0001	-0.0002	-0.0003	0.0022
Bkgd Syst	$\pm^{0.0000}_{0.0000}$	$\pm^{0.0000}_{0.0001}$	$\pm^{0.0000}_{0.0000}$	$\pm^{0.0001}_{0.0001}$	$\pm^{0.0008}_{0.0009}$	$\pm^{0.0013}_{0.0013}$	$\pm^{0.0013}_{0.0012}$

Table 14: A_3 central value and uncertainties for $|y| < 1.0$ from 1D fit result.

γ^*/ZP_T; $1.0 \leq \lvert Y \rvert < 2.4$	0–10	10–20	20–35	35–55	55–80	80–120	120–200
A3 Central Value	-0.0089	-0.0018	-0.0071	-0.0067	0.0076	-0.0018	0.0180
Stat. Uncert.	0.0050	0.0059	0.0075	0.0110	0.0171	0.0261	0.0420
Syst. Uncert.	$\pm^{0.0069}_{0.0069}$	$\pm^{0.0053}_{0.0053}$	$\pm^{0.0036}_{0.0036}$	$\pm^{0.0032}_{0.0032}$	$\pm^{0.0040}_{0.0040}$	$\pm^{0.0045}_{0.0046}$	$\pm^{0.0110}_{0.0115}$
PU Syst	$\pm^{0.0001}_{0.0001}$	$\pm^{0.0006}_{0.0005}$	$\pm^{0.0000}_{0.0000}$	$\pm^{0.0004}_{0.0001}$	$\pm^{0.0000}_{0.0001}$	$\pm^{0.0005}_{0.0013}$	$\pm^{0.0010}_{0.0015}$
Mom. Corr. Syst	0.0069	0.0053	0.0036	0.0032	0.0040	0.0037	0.0056
TnP Syst	0.0001	0.0001	0.0001	0.0001	0.0002	0.0003	0.0006
Z P_T Syst	0.0003	0.0000	0.0002	0.0000	0.0004	0.0001	0.0004
Bkgd Syst	$\pm^{0.0001}_{0.0002}$	$\pm^{0.0001}_{0.0001}$	$\pm^{0.0002}_{0.0002}$	$\pm^{0.0003}_{0.0003}$	$\pm^{0.0006}_{0.0006}$	$\pm^{0.0024}_{0.0023}$	$\pm^{0.0093}_{0.0099}$

Table 15: A_3 central value and uncertainties for $1.0 \leq |y| < 2.4$ from 1D fit result.

γ^*/ZP_T; $0.0 \leq \lvert Y \rvert < 1.0$	0–10	10–20	20–35	35–55	55–80	80–120	120–200
A4 Central Value	0.0179	0.0071	0.0165	0.0333	-0.0029	-0.0158	-0.0042
Stat. Uncert.	0.0039	0.0055	0.0073	0.0104	0.0140	0.0178	0.0259
Syst. Uncert.	$\pm^{0.0004}_{0.0004}$	$\pm^{0.0022}_{0.0022}$	$\pm^{0.0012}_{0.0012}$	$\pm^{0.0012}_{0.0012}$	$\pm^{0.0014}_{0.0014}$	$\pm^{0.0016}_{0.0014}$	$\pm^{0.0028}_{0.0027}$
PU Syst	$\pm^{0.0002}_{0.0003}$	$\pm^{0.0005}_{0.0004}$	$\pm^{0.0001}_{0.0002}$	$\pm^{0.0007}_{0.0008}$	$\pm^{0.0001}_{0.0000}$	$\pm^{0.0009}_{0.0004}$	$\pm^{0.0017}_{0.0015}$
Mom. Corr. Syst	0.0003	0.0021	0.0011	0.0008	0.0013	0.0012	0.0020
TnP Syst	0.0001	0.0001	0.0001	0.0001	0.0002	0.0002	0.0002
Z P_T Syst	0.0001	0.0001	0.0001	0.0000	0.0000	0.0006	0.0010
Bkgd Syst	$\pm^{0.0001}_{0.0001}$	$\pm^{0.0001}_{0.0001}$	$\pm^{0.0002}_{0.0002}$	$\pm^{0.0003}_{0.0003}$	$\pm^{0.0005}_{0.0005}$	$\pm^{0.0002}_{0.0002}$	$\pm^{0.0004}_{0.0004}$

Table 16: A_4 central value and uncertainties for $|y| < 1.0$ from 1D fit result.

γ^*/ZP_T; $1.0 \leq \lvert Y \rvert < 2.4$	0–10	10–20	20–35	35–55	55–80	80–120	120–200
A4 Central Value	0.0726	0.0761	0.0614	0.0524	0.0391	0.0665	0.0268
Stat. Uncert.	0.0052	0.0071	0.0094	0.0138	0.0190	0.0228	0.0320
Syst. Uncert.	$\pm^{0.0007}_{0.0007}$	$\pm^{0.0009}_{0.0009}$	$\pm^{0.0015}_{0.0015}$	$\pm^{0.0029}_{0.0029}$	$\pm^{0.0024}_{0.0025}$	$\pm^{0.0037}_{0.0033}$	$\pm^{0.0051}_{0.0050}$
PU Syst	$\pm^{0.0003}_{0.0003}$	$\pm^{0.0003}_{0.0003}$	$\pm^{0.0001}_{0.0001}$	$\pm^{0.0025}_{0.0026}$	$\pm^{0.0009}_{0.0011}$	$\pm^{0.0022}_{0.0014}$	$\pm^{0.0022}_{0.0018}$
Mom. Corr. Syst	0.0006	0.0008	0.0015	0.0013	0.0022	0.0023	0.0035
TnP Syst	0.0001	0.0001	0.0001	0.0001	0.0001	0.0002	0.0004
Z P_T Syst	0.0001	0.0000	0.0000	0.0000	0.0001	0.0006	0.0014
Bkgd Syst	$\pm^{0.0000}_{0.0001}$	$\pm^{0.0004}_{0.0004}$	$\pm^{0.0001}_{0.0000}$	$\pm^{0.0001}_{0.0001}$	$\pm^{0.0001}_{0.0001}$	$\pm^{0.0017}_{0.0018}$	$\pm^{0.0026}_{0.0027}$

Table 17: A_4 central value and uncertainties for $1.0 \leq |y| < 2.4$ from 1D fit result.

DRAFT